J Mater Sci (2023) 58:10677–10685

Electronic materials

Orbital hybridization and polarization resistance of Cu-doped $PrBaCo_2O_{5+\delta}$

Kanghee Jo[1], Jiseung Ryu[2], Ilguk Jo[3], and Heesoo Lee[1,*]

[1] Present address: Department of Materials Science and Engineering, Pusan National University, Busan 46241, Republic of Korea
[2] Analysis Technology Center, Korea Institute of Ceramic Engineering and Technology, Jinju 52851, Republic of Korea
[3] Division of Advanced Materials Engineering, Dong-Eui University, Busan 47340, Republic of Korea

Received: 19 February 2023
Accepted: 15 June 2023
Published online: 28 June 2023

ABSTRACT

The effects of Cu doping of $PrBaCo_2O_{5+\delta}$ layered perovskite oxide (PBCCux, x = 0, 0.1, 0.2, and 0.5) were investigated in terms of local atomic structure change and polarization resistance. As the copper doping concentration in PBCCux increased, the peaks in the XRD patterns of the samples shifted to lower angle which indicates lattice expansion by oxygen vacancy formation and larger ion doping. O K-edge XANES was used to determine the change in orbital hybridization with Cu doping, and it was confirmed that the O^{2-} species decreased and the monoxidic species increased with the addition of Cu resulting in covalency increase. As the Cu content increased, the Co–O first shell intensity decreased in the Co K-edge EXAFS spectra because of the formation of oxygen vacancies by Cu doping. The impedance at 600 °C decreased by approximately 73% from 0.91 Ω cm^2 (PBCO) to 0.23 Ω cm^2 (PBCCu0.5) by the synergetic effect of oxygen vacancy formation and the increase in covalency.

Introduction

Solid oxide fuel cells (SOFC) are promising energy conversion systems that directly convert chemical energy into electrical energy and exhibit a high energy conversion efficiency of over 80%. The high operating temperature of 800–1000 °C induces challenges in selecting surrounding materials and accelerates their deterioration [1, 2]. Research on lowering the operating temperature to 500–800 °C is actively being conducted. Mixed ionic-electronic conductors (MIECs) have received considerable attention as promising cathode materials capable of achieving high performance for intermediate temperature SOFCs (IT-SOFCs, below 800 °C). Perovskite oxides have attracted attention as cathode materials for SOFC/SOECs because of their excellent electrochemical properties and mixed ionic electronic conductivity. Various methods such as transition metal doping, infiltration, and exsolution have been used,

Handling Editor: Till Froemling.

Address correspondence to E-mail: heesoo@pusan.ac.kr
E-mail Addresses: jokanghee@pusan.ac.kr; jsryu@kicet.re.kr; ijo@deu.ac.kr

https://doi.org/10.1007/s10853-023-08699-7

and layered perovskite oxides using cation ordering have also been studied to improve the electrocatalytic activity of perovskite oxides [3, 4].

The layered perovskite oxide ($AA'B_2O_{5+\delta}$) has a structure in which $[BO_2]$–$[AO_\delta]$–$[BO_2]$–$[A'O]$ layers are continuously stacked along the c-axis of the lattice. This layered structure reduces the oxygen-binding force of the $[AO_\delta]$ layer and effectively improves the diffusion of oxygen ions by forming an oxygen pathway [5]. The electrochemical properties of perovskite oxides are determined by various factors such as B–O covalency, O p-band center, charge transfer energy, and valence band structure resulting from the crystal structure and electronic structure. Lee et al. predicted the ORR catalytic activity of SOFCs by comparing them with measurable indicators, such as the O p-band center, polarization resistance, and surface exchange constant, paying attention to the importance of oxygen conduction [6].

$LnBaCo_2O_{5+\delta}$ (Ln = Pr, Nd, Sm, etc.) has been reported to exhibit excellent electrical conductivity, fast surface oxygen exchange, and high oxygen-ion conductivity [7]. Kim et al. showed that $PrBaCo_2O_{5+d}$ have over 1000 S/cm of electrical conductivity below 600 °C, the order of 10^{-4} cm^2/s bulk diffusion and the order of 10^{-2} cm/s surface exchange coefficient using ECR and IEDP. These values are the best values among perovskite oxide-based oxides and are the same or better values about 500 °C lower than conventional LSC and LSF. This is the result of the cation ordering and high oxygen vacancy concentration that occur during the formation of PBCO, and the ease of changing the oxidation rate of Co ions [8]. To improve polarization resistance in these PBCOs in various studies, a number of studies on doping with Fe, Cu, Sr, etc., have been conducted. When Cu was doped, the electrical conductivity tended to decrease slightly, but the polarization resistance was reduced by about 30–50%. Studies conducted by Jin et al., Zhao et al. and Suntsov et al. discussed the main reasons for polarization resistance reduction were the increase in Co^{3+}/Co^{4+}, Cu^{+}/Cu^{2+} reduction pairs, and the increase in oxygen vacancies due to Cu doping. B–O covalency, op-band center, charge transfer energy, and valence band structure suggested above have been discussed in some studies, but research on the interaction between orbitals and the change in band structure according to doping is needed [9–11].

In a previous study, we observed the effect of changes in the oxidation number and valence band structure of $PrBaCo_{2-x}Cu_xO_{5+\delta}$ (PBCCux) layered perovskite samples according to Cu doping on the reduction of polarization resistance [12]. Herein, the changes in the local atomic structure and orbital hybridization with Cu doping were analyzed. Co K-edge EXAFS was used to analyze the crystal structure and consequent local structural changes, and O K-edge XANES was used to analyze changes in orbital hybridization.

Materials and methods

Powder synthesis

PBCO ($PrBaCo_2O_{5+\delta}$) and PBCCux ($PrBaCo_{2-x}Cu_xO_{5+\delta}$, x = 0.1, 0.2, 0.5) powders were synthesized using an EDTA-citrate complexing process. $Pr(NO_3)_3{\cdot}6H_2O$ (99.9%, Sigma-Aldrich), $Co(NO_3)_3{\cdot}6H_2O$, $Cu(NO_3)_2{\cdot}2.5H_2O$ (98%, Sigma-Aldrich), and $Ba(NO_3)_2$ (99%+, Alfa Aesar) metal precursors were dissolved in deionized water. EDTA (99.5%, Alfa Aesar) was added to 1 N NH_4OH (Junsei Chemical Co.) solution to obtain an NH_3-EDTA buffer solution. The NH_3-EDTA solution and crystallized citric acid (99.5%, Samchun Chemical) powders were added to the metal precursor solution to make a sol with a total metal ion/EDTA/citric acid molar ratio of 1:1:2. The solution was heated to 75 °C while adjusting the pH to 9 using NH_4OH, and the solvent was evaporated to obtain clear gels. These gels were pre-calcined at 450 °C and calcined in air at 950 °C.

Symmetric cell preparation

Symmetric cells (PBCCux | SDC | PBCCux) were prepared to investigate the electrochemical properties of the PBCCu. The SDC pellets were sintered at 1400 °C for 4 h using SDC powder (SDC20-HP, Fuelcellmaterials). The PBCCu powders were mixed with a binder prepared from α-terpineol and ethylcellulose to form PBCCu pastes, which were screen-printed onto both sides of the SDC pellets. After drying, the symmetric cells were calcined at 950 °C for 2 h in air.

Characterization

To examine the crystal structures of the calcined and sintered powders, powder X-ray diffraction (XRD, PANalytical X'pert-Pro MPD PW3040/60) was

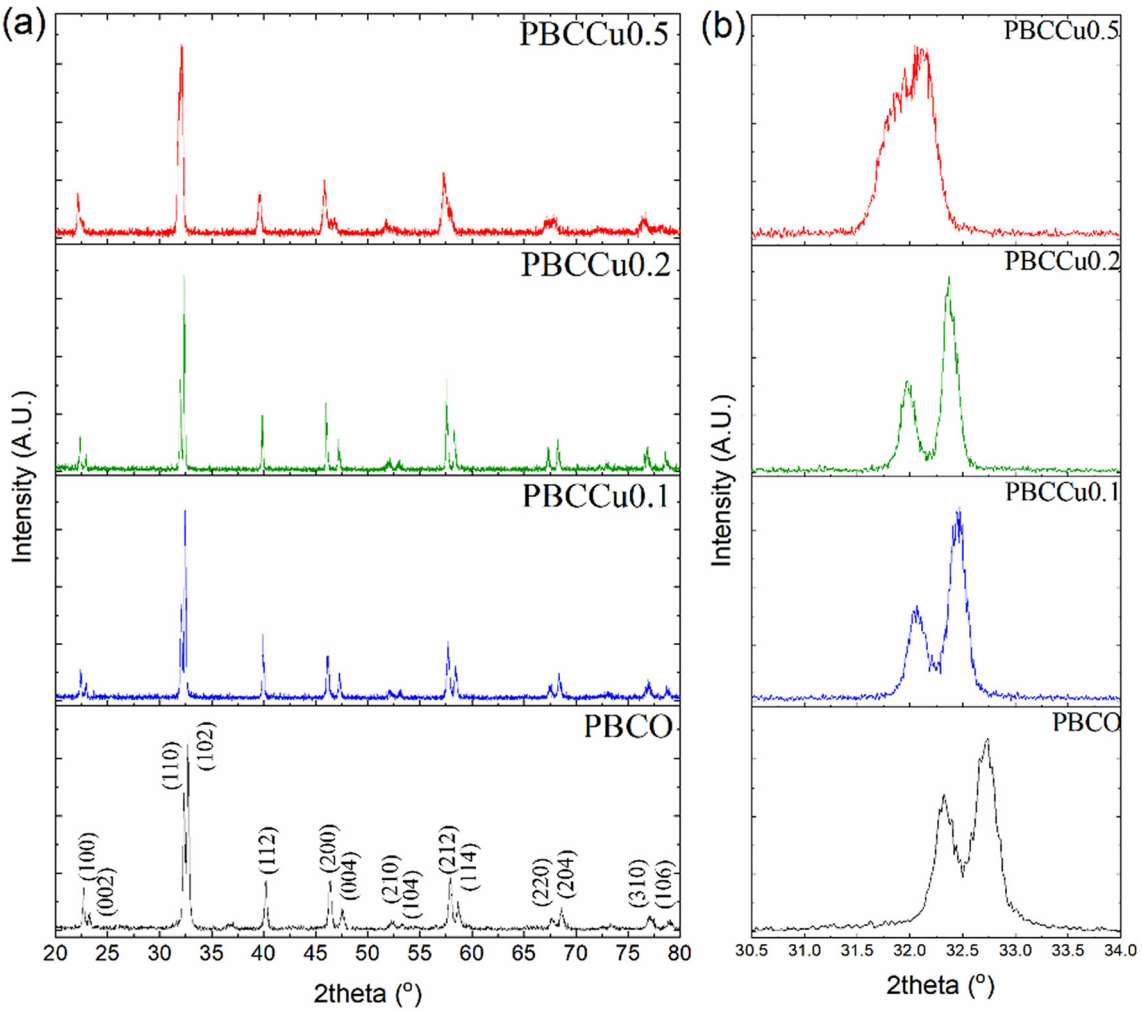

Figure 1 **a** X-ray diffraction pattern **b** main peak around 32° of PBCO and PBCCux layered perovskite oxide.

performed at room temperature using a step scan procedure (0.02°/2θ step, time per step 0.5 s) in the 2θ range of 10°–90°. O K edge NEXAFS and Co K edge XAS analysis was performed at the PLS-II 4D beamline (base pressure 3.0×10^{-10} Torr) and 10C beamline in the Pohang Accelerator Laboratory (PAL, Republic of Korea). XAS analysis was performed using the IFEFFIT interactive software package (with ATHENA graphical interfaces). Background subtraction was processed by fitting linear polynomials to the pre-edge and the post-edge region of an absorption spectrum, respectively. The $v(E)$ data were converted into k-space, k-weighted, and Fourier transformed using a Hanning window, into r-space.

Impedance measurements were conducted using an IviumStat instrument (Ivium, the Netherlands) over the frequency range of 10^6–0.01 Hz with an excitation voltage of 10 mV at an operating temperature of 600–700 °C under open-circuit conditions in air. The electrochemical impedance spectroscopy results were multiplied by 0.5 to account for the two electrodes. The impedance spectra data were further fitting by an EC-lab software. Distribution of relaxation time (DRT) method was applied to analyze the EIS data.

Results and discussion

Figure 1a shows the XRD pattern of Cu-doped PBCO. All compositions showed an orthorhombic structure, and secondary phases, including CuO, were not observed in PBCCux. Each peak of $PrBaCo_2O_{5+\delta}$ (PBCO), which is the basic composition, was indexed according to the *P4/mmm* structure. The peak position shifted to a lower angle according to the Cu content

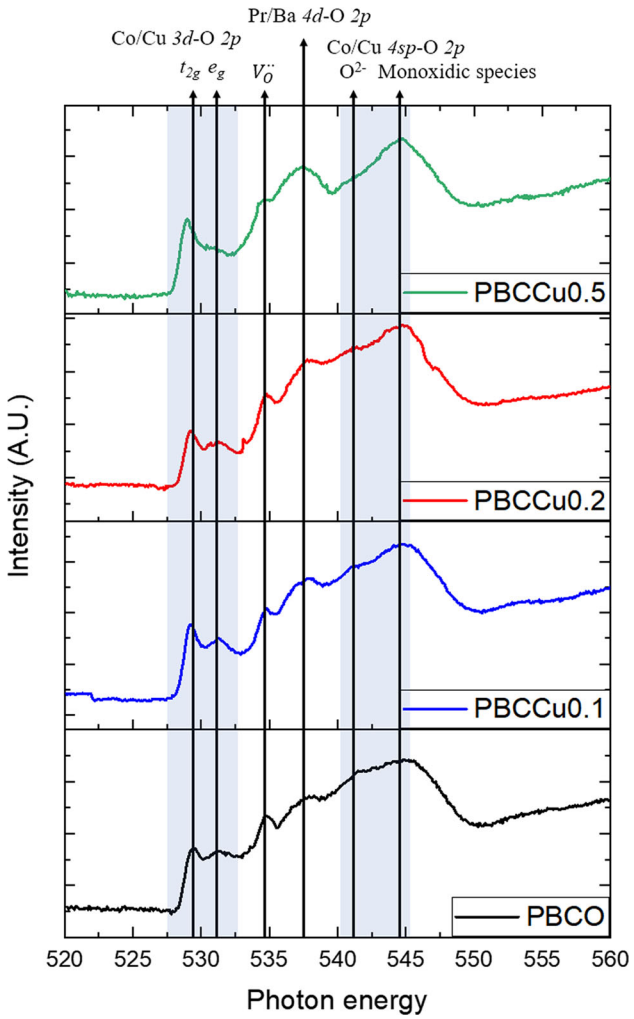

Figure 2 Normalized O K-edge NEXAFS spectra of the layered perovskite-type PBCO, PBCCu0.1, PBCCu0.2 and PBCCu0.5 powder.

as shown in Fig. 1b. This is a chemical expansion caused by the expansion of the lattice by replacing Co^{3+} ions (61 pm) with Cu^{2+} (73 pm). Oxygen vacancy concentration is increased due to the B site oxidation state reduction from 3.26 (PBCO) to 2.90 (PBCCu0.5) as shown in Figure S1 and Table S1. The lattice free volume increases due to the synergetic effect of lattice expansion by chemical expansion and oxygen vacancy formation and oxygen ion mobility increases accordingly [12–14].

Figure 2 shows the entire O K-edge XAS spectra of the PBCCux powder to investigate the electronic structure change, which is affected by the addition of Cu. The peaks in the 527–532 eV region originate from the interaction between the unoccupied state of the Co/Cu 3d orbital; the peak in the 535 eV region is a peak formed by reflection by oxygen vacancies; the peak formed in the 537.5 eV region is attributed to the hybridization of the Pr/Ba 4d orbital and O 2p orbital; the peaks in the 540–545 eV region are formed by the hybridization of Co/Cu 4sp and O 2p orbitals; the 541 eV region is due to O^{2-} during the hybridization of Co/Cu 4sp and O 2p orbitals; and the peaks in the 544 eV region are Co/Cu 4sp and O 2p orbitals. It has been reported that the hybridization of Cu 4sp and O 2p orbitals is caused by monoxidic species [15–22].

The pre-edge peaks are 529.5 529.3 529.2 and 529.0 eV for PBCO, PBCCu0.1, PBCCu0.2, PBCCu0.5, respectively. It has been reported that the shift of the pre-edge peak to a lower energy is due to the increased covalency of Co–O. The O 2p ligand holes were split into two peaks, indicating the e_g and t_{2g} orbitals, by crystal field splitting. With the addition of Cu, the intensity ratio of the two orbitals formed by the crystal field splitting ($I_{t_{2g}}/I_{e_g}$) gradually increased. This is because as the Cu content increased, Co^{3+} with a $3d^6$ electron configuration was replaced with Cu^{2+} with a $3d^9$ electron configuration, and the number of electrons in the t_{2g} orbital gradually increased as shown in Fig. 3. The peak due to Pr/Ba 4d–O 2p hybridization did not shift at 535 eV because the hybridization of the A-site cation and O anion did not change. The O^{2-} peak gradually decreases, and the monoxidic species peak gradually increases in the peak due to Co/Cu 4sp–O 2p hybridization. This corresponds to the fact that the covalency increased, as in the previous pre-edge peak shift [23].

Figure 4a shows the Co K-edge XAS spectrum, and (b) shows the pre-edge structure of the Co K-edge. As Cu was added to the pre-edge structure, the ratio of the t_{2g} orbital increased. This is because the number of electrons corresponding to the t_{2g} orbital is increased by Cu doping, as previously confirmed by O K-edge XANES.

Figure 4c, d shows the EXAFS $k^3\chi$ spectrum and Fourier transformed EXAFS spectra (R space) of the Co K-edge of PBCO and PBCCux. The first peak is formed by the nearest neighbor, and the second peak in the 2.8 Å is formed by Co–Co/Cu bonding. The first shell intensity gradually decreased with increasing Cu content, which corresponds to a decrease in the Co–O coordination shell due to the formation of oxygen vacancies according to Cu doping [24, 25]. The peak around 3.0 Å was formed

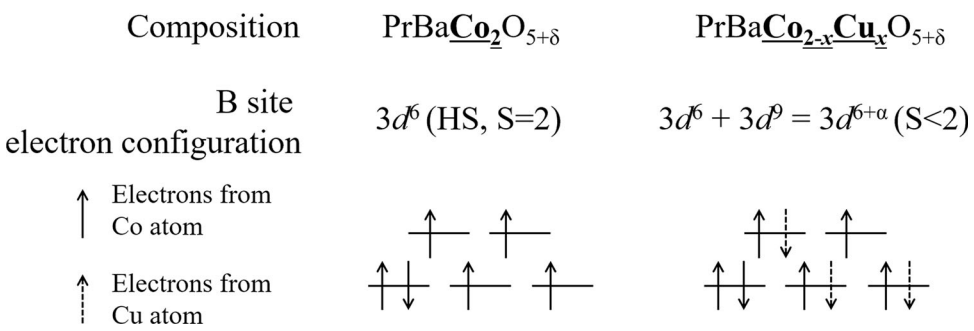

Figure 3 Comparison of electron configuration of PBCO and PBCCux.

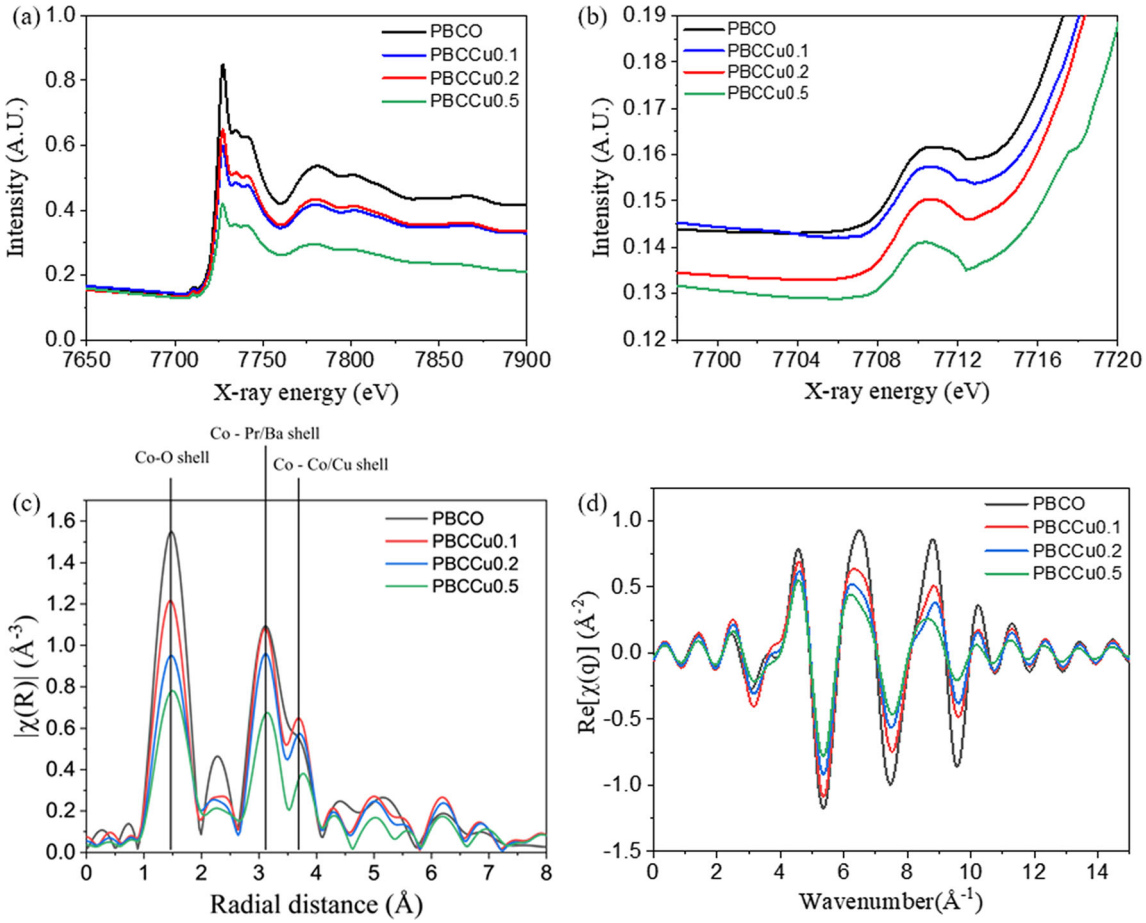

Figure 4 **a** Co K edge XAS spectra **b** XANES spectra in the range of 7698–7720 eV **c** Fourier transform of Co K-edge EXAFS $k^3\chi$ data and **d** EXAFS $k^3\chi$ data at Co K-edge of PBCCux powders at room temperature (k range from 2 to 12.5 $Å^{-1}$).

by the adjacent Pr/Ba. The second and third peaks are due to the Co-Pr/Ba shell and corner shared CoO_6 octahedron, respectively, and similar to the fingerprint of the perovskite structure [26].

Figure 5a shows the electrochemical impedance spectra (EIS) measured at 600–700 °C for the symmetric cell of the PBCCux electrode. The polarization resistance was calculated by measuring the distance between the intercepts of Z′ when Z″ is equal to 0. The polarization resistances of PBCCux were 0.91 Ω cm^2 (PBCO), 0.60 Ω cm^2 (PBCCu0.1), 0.47 Ω cm^2 (PBCCu0.2) and 0.23 Ω cm^2 (PBCCu0.5) and gradually decreased as Cu was doped, so that PBCCu0.5 showed a 74.72% smaller value compared to that of PBCO. In addition, the activation energy was calculated at 600–700 °C and is shown in Table 1. Arrhenius dependence was observed in all compositions, and the activation energy decreased

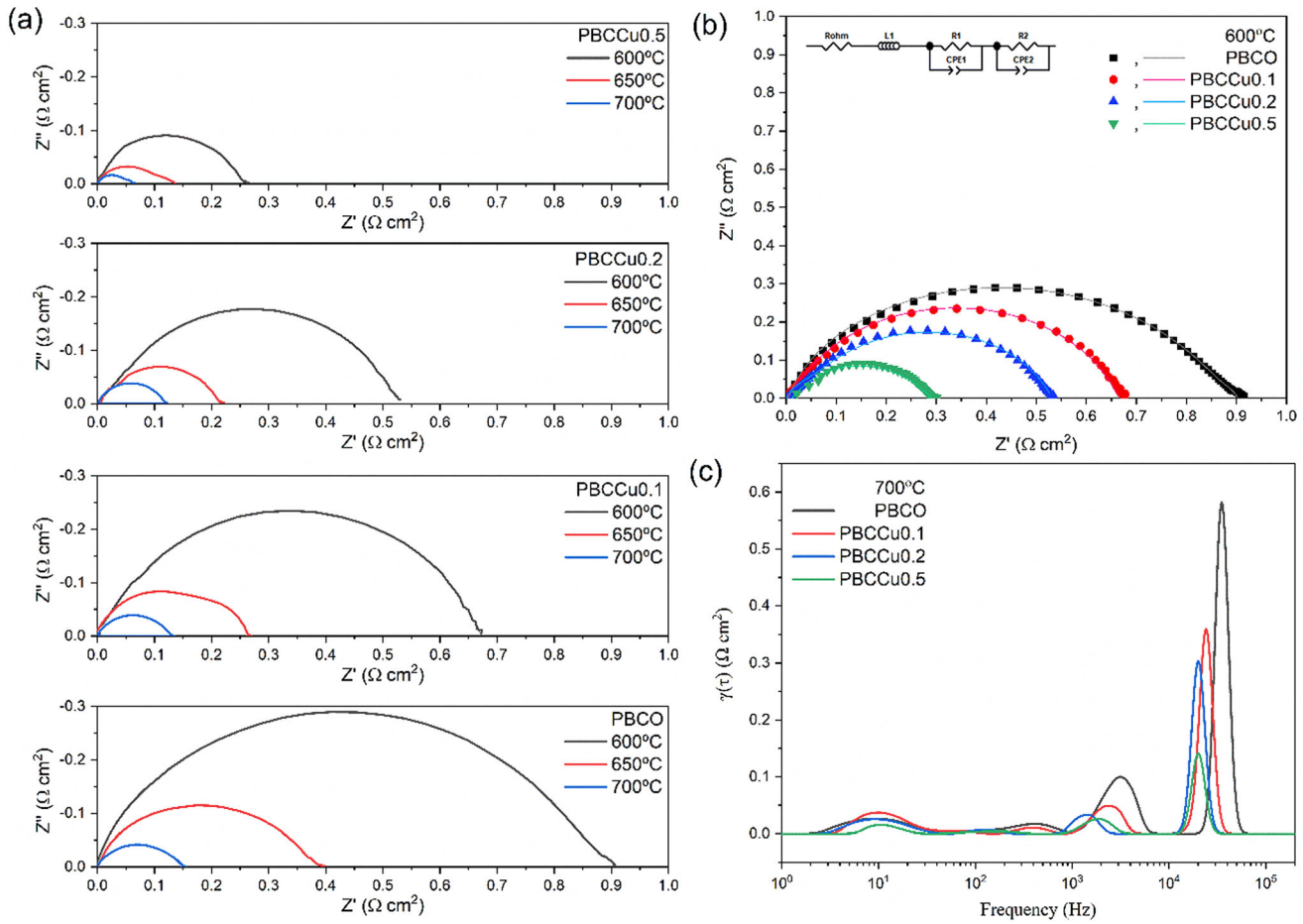

Figure 5 **a** Nyquist plot of PBCCux in air at 600–700 °C **b** example of fitting at 600 °C R_{ohm} was subtracted to emphasize the polarization resistance and observed data and fitted data are shown as dots and solid line, respectively, and **c** DRT curves of EIS at 700 °C.

Table 1 Polarization resistance and activation energy for PBCCux at 600–700 °C

Sample name	Polarization resistance (Ω cm^2)			Activation energy (eV)
	600 °C	650 °C	700 °C	
PBCO	0.91	0.40	0.15	1.299
PBCCu0.1	0.67	0.26	0.13	1.191
PBCCu0.2	0.53	0.22	0.12	1.120
PBCCu0.5	0.26	0.14	0.06	1.034

gradually as the Cu doping concentration increased, with the smallest value being observed in PBCCu0.5.

EIS fitting using equivalent circuit and distribution of relaxation time (DRT) analysis conducted for better understanding of the ORR process. The impedance spectra were fitted using series of two ZARC element as shown in Fig. 5b and two distinctive peaks in DRT were observed in around 10^5 Hz, 10^3 Hz and 10 Hz in Fig. 5c. Both peaks shifted to lower frequency with Cu content increasing, while 10 Hz peak remains same position. According to the literature, the high frequency (> 10^3 Hz), intermediate frequency (1–10^3 Hz) and low frequency (10^{-2} to 1 Hz) characteristic peaks are related to oxygen ion charge transfer from electrolyte to cathode at TPB, surface exchange or ion transfer at cathode and gas diffusion process, respectively. As Cu was doped, it was found that the oxygen ion transfer and surface electron exchange in TPB were accelerated, and the impedance decreased. The doping of Cu accelerated

oxygen ion transfer and surface electron exchange at TPB, which decreased the impedance [27].

The doping of Cu in PBCO improves the electrochemical properties. This is because the doping of Cu increases the number of oxygen vacancies in the lattice and the free volume of the lattice, which improves the mobility of oxygen ions. In addition, the improvement of B–O bond covalency due to the change in B–O bond structure and orbital hybridization accelerates surface electron exchange and oxygen ion transfer at TPB.

Conclusion

We investigated the orbital hybridization and the polarization resistance changes of $PrBaCo_2O_{5+\delta}$ doped with Cu (PBCCux, x = 0.1, 0.2, and 0.5). O K-edge XANES analysis confirmed that the lower energy shift of the pre-edge peak and the covalency of the Co–O bond increased by decreasing the O^{2-} species and increasing the monoxidic species in the lower energy shift of the pre-edge peak and the Co/Cu 4sp–O 2p hybridization. Co K-edge EXAFS analysis indicated that the Co–O first shell intensity decreased as the Cu content increased, which was due to the formation of oxygen vacancies by Cu doping. With an increase in the Cu content, the impedance decreased by approximately 73% from 0.91 Ω cm^2 (PBCO) to 0.23 Ω cm^2 (PBCCu0.5) at 600 °C due to the synergetic effect of the increase in oxygen vacancies in the lattice along with the increase in the covalency of B–O bonds.

Acknowledgements

This work was supported by Korea Institute for Advancement of Technology grant funded by the Korea Government (MOTIE) (P0008335, The Competency Development Program for Industry specialist).

Author contributions

Kanghee Jo was involved in conceptualization, Writing—original draft; Jiseung Ryu contributed to investigation, writing—original draft; Ilguk Jo was involved in writing—review and editing; Heesoo Lee contributed to supervision, writing—review and editing.

Data availability

Not applicable.

Declarations

Conflict of interest The authors declare they have no conflict of interest.

Ethical approval No experiments involving human tissue were conducted in current study.

Supplementary Information: The online version contains supplementary material available at https://doi.org/10.1007/s10853-023-08699-7.

References

[1] Jiang L, Wei T, Zeng R, Zhang WX, Huang YH (2013) Thermal and electrochemical properties of PrBa0. 5Sr0. $5Co_{2-x}FexO_{5+\delta}$ (x = 0.5, 1.0, 1.5) cathode materials for solid-oxide fuel cells. J Power Sources 232:279–285. https://doi.org/10.1016/j.jpowsour.2013.01.064

[2] Zhu C, Liu X, Yi C, Yan D, Su W (2008) Electrochemical performance of $PrBaCo_2O_{5+\delta}$ layered perovskite as an intermediate-temperature solid oxide fuel cell cathode. J Power Sources 185(1):193–196. https://doi.org/10.1016/j.jpowsour.2008.06.075

[3] Pelosato R, Cordaro G, Stucchi D, Cristiani C, Dotelli G (2015) Cobalt based layered perovskites as cathode material for intermediate temperature solid oxide fuel cells: a brief review. J Power Sources 298:46–67. https://doi.org/10.1016/j.jpowsour.2015.08.034

[4] Wang B, Long G, Ji Y, Pang M, Meng X (2014) Layered perovskite $PrBa_{0.5}Sr_{0.5}CoCuO_{5+\delta}$ as a cathode for intermediate-temperature solid oxide fuel cells. J Alloys Compd 606:92–96. https://doi.org/10.1016/j.jallcom.2014.03.138

[5] Jun A, Kim J, Shin J, Kim G (2016) Perovskite as a cathode material: a review of its role in solid-oxide fuel cell technology. ChemElectroChem 3(4):511–530. https://doi.org/10.1002/celc.201500382

[6] Lee YL, Kleis J, Rossmeisl J, Shao-Horn Y, Morgan D (2011) Prediction of solid oxide fuel cell cathode activity with first-principles descriptors. Energy Environ Sci 4(10):3966–3970. https://doi.org/10.1039/C1EE02032C

[7] Verduzco LE, Garcia-Díaz R, Martinez AI, Salgado RA, Méndez-Arriaga F, Lozano-Morales SA, Avendano-Alejo M, Padmasree KP (2020) Degradation efficiency of methyl orange dye by $La_{0.5}Sr_{0.5}CoO_3$ perovskite oxide under dark and UV irradiated conditions. Dyes Pigm 183:108743. https://doi.org/10.1016/j.dyepig.2020.108743

[8] Kim G, Wang S, Jacobson AJ, Reimus L, Brodersen P, Mims CA (2007) Rapid oxygen ion diffusion and surface exchange kinetics in $PrBaCo_2O_{5+x}$ with a perovskite related structure and ordered A cations. J Mater Chem 17(24):2500–2505. https://doi.org/10.1039/B618345J

[9] Jin F, Shen Y, Wang R, He T (2013) Double-perovskite $PrBaCo_{2/3}Fe_{2/3}Cu_{2/3}O_{5+\delta}$ as cathode material for intermediate-temperature solid-oxide fuel cells. J Power Sources 234:244–251. https://doi.org/10.1016/j.jpowsour.2013.01.172

[10] Zhao L, Nian Q, He B, Lin B, Ding H, Wang S et al (2010) Novel layered perovskite oxide $PrBaCuCoO_{5+\delta}$ as a potential cathode for intermediate-temperature solid oxide fuel cells. J Power Sources 195(2):453–456. https://doi.org/10.1016/j.jpowsour.2009.08.009

[11] Suntsov AY, Leonidov IA, Markov AA, Patrakeev MV, Blinovskov YN, Kozhevnikov VL (2009) Oxygen nonstoichiometry and the thermodynamic and structural properties of double perovskites $PrBaCo_{2-x}Cu_xO_{5+\delta}$. Russ J Phys Chem A 83:832–838. https://doi.org/10.1134/S0036024409050264

[12] Jo K, Kim T, Ryu J, Noh T, Lee H (2020) Valence band structure and oxygen reduction reaction of Cu doped $PrBaCo_2O_{5+\delta}$. Mater Lett 277:128399. https://doi.org/10.1016/j.matlet.2020.128399

[13] Chen H, Lim C, Zhou M, He Z, Sun X, Li X, Ye Y, Tan T, Zhang H, Yang C, Han J, Chen Y (2021) Activating lattice oxygen in perovskite oxide by B-site cation doping for modulated stability and activity at elevated temperatures. Adv Sci 8(22):2102713. https://doi.org/10.1002/advs.202102713

[14] Li Z, Li M, Zhu Z (2022) Perovskite cathode materials for low-temperature solid oxide fuel cells: fundamentals to optimization. Electrochem Energy Rev 5(2):263–311. https://doi.org/10.1007/s41918-021-00098-3

[15] Suntsov AY, Leonidov IA, Patrakeev MV, Kozhevnikov VL (2015) Defect formation in double perovskites $PrBaCo_{2-x}Cu_xO_{5+\delta}$ at elevated temperatures. Solid State Ion 274:17–23. https://doi.org/10.1016/j.ssi.2015.02.004

[16] Wang X, Huang K, Yuan L, Xi S, Yan W, Geng Z, Cong Y, Sun Y, Tan H, Wu X, Li L, Feng S (2018) Activation of surface oxygen sites in a cobalt-based perovskite model catalyst for CO oxidation. J Phys Chem Lett 9(15):4146–4154. https://doi.org/10.1021/acs.jpclett.8b01623

[17] Tafaroji S, Farbod M, Kazeminezhad I, Kheirmand M (2019) Effect of pre-sintering temperature and ball-milling on the conductivity of $Ba_{0.5}Sr_{0.5}Co_{0.8}Fe_{0.2}O_{3-\delta}$ as a cathode for solid oxide fuel cells prepared by sol–gel thermolysis method. *Mater Res Express* 6(9):095522. https://doi.org/10.1088/2053-1591/ab3265

[18] Mueller DN, Machala ML, Bluhm H, Chueh WC (2015) Redox activity of surface oxygen anions in oxygen-deficient perovskite oxides during electrochemical reactions. Nat Commun 6(1):1–8. https://doi.org/10.1038/ncomms7097

[19] Padilla-Pantoja J, Herrero-Martín J, Gargiani P, Valvidares SM, Cuartero V, Kummer K, Watson O, Brookes NB, García-Muñoz JL (2014) Stability of the cationic oxidation states in $Pr_{0.50}Sr_{0.50}CoO_3$ across the magnetostructural transition by X-ray absorption spectroscopy. Inorg Chem 53(17):8854–8858. https://doi.org/10.1021/ic403117j

[20] Suntivich J, Hong WT, Lee YL, Rondinelli JM, Yang W, Goodenough JB, Dabrowski B, Freeland WJ, Shao-Horn Y (2014) Estimating hybridization of transition metal and oxygen states in perovskites from Ok-edge X-ray absorption spectroscopy. J Phys Chem C 118(4):1856–1863. https://doi.org/10.1021/jp410644j

[21] Li X, Sun Y, Ren F, Bai Y, Cheng Z (2021) Smart oxygen vacancy engineering to enhance water oxidation efficiency by separating the different effects of bulk and surface vacancies. Mater Today Energy 19:100619. https://doi.org/10.1016/j.mtener.2020.100619

[22] Zhao J, Liu C, Li J, Wu R, Wang J, Qian H, Guo H, Li J, Ibrahim K (2019) Oxygen vacancy induced electronic structure variation in the $La_{0.2}Sr_{0.8}MnO_3$ thin film. AIP Adv 9(5):055208. https://doi.org/10.1063/1.5088738

[23] Karvonen L, Valkeapaa M, Liu RS, Chen JM, Yamauchi H, Karppinen M (2010) O-K and Co-L XANES study on oxygen intercalation in perovskite $SrCoO_{3-\delta}$. Chem Mater 22(1):70–76. https://doi.org/10.1021/cm9021563

[24] Luo Y, Zheng Y, Feng X, Lin D, Qian Q, Wang X, Zhang Y, Chen Q, Zhang X (2020) Controllable P doping of the $LaCoO_3$ catalyst for efficient propane oxidation: optimized surface Co distribution and enhanced oxygen vacancies. ACS Appl Mater Interfaces 12(21):23789–23799. https://doi.org/10.1021/acsami.0c01599

[25] Kriventsov VV, Kochubey DI, Ismagilov ZR, Podyacheva OY, Nemudry AP (2005) EXAFS study of Nb doped Sr(Co/Fe)O_{3-x} perovskites. Phys Scr T115:740. https://doi.org/10.1238/Physica.Topical.115a00740

[26] Risch M, Grimaud A, May KJ, Stoerzinger KA, Chen TJ, Mansour AN, Shao-Horn Y (2013) Structural changes of cobalt-based perovskites upon water oxidation investigated

by EXAFS. J Phys Chem C 117(17):8628–8635. https://doi.org/10.1021/jp3126768

[27] Yang Q, Tian D, Liu R, Wu H, Chen Y, Ding Y et al (2021) Exploiting rare-earth-abundant layered perovskite cathodes of $LnBa_{0.5}Sr_{0.5}Co_{1.5}Fe_{0.5}O_{5+\delta}$ (Ln = La and Nd) for SOFCs. Int J Hydrog Energy 46(7):5630–5641. https://doi.org/10.1016/j.ijhydene.2020.11.031